



Electromagnetic response of graphene and role of evanescent waves in resolution of the Casimir puzzle

G. L. Klimchitskaya and V. M. Mostepanenko

Central Astronomical Observatory at Pulkovo
of the Russian Academy of Sciences, Saint Petersburg, Russia
and
Peter the Great Saint Petersburg Polytechnic University,
Saint Petersburg, Russia

Pulkovo Observatory



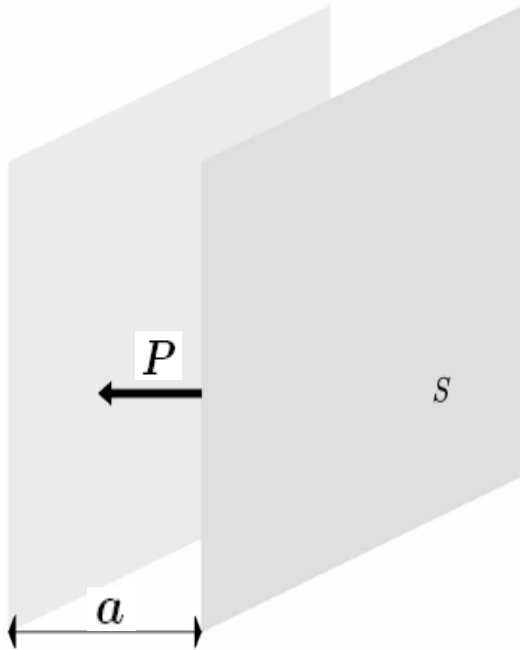
CONTENT



- 1. Introduction**
- 2. Response functions of graphene at low energies**
- 3. Casimir force in graphene systems**
- 4. Agreement between experiment and theory for graphene systems**
- 5. Agreement with the requirements of thermodynamics**
- 6. What is the Casimir puzzle for metallic plates?**
- 7. The role of s-polarized evanescent waves in the Casimir puzzle**
- 8. The lessons of graphene for the Casimir effect**
- 9. How to test the Drude model in the range of s-polarized evanescent waves**
- 10. Conclusions**



1. INTRODUCTION



For ideal metal plates

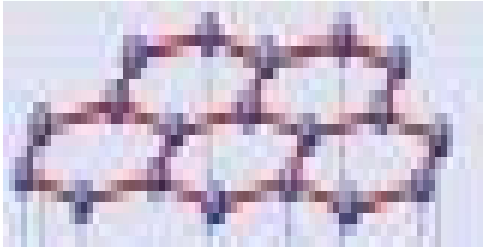
$$P = -\frac{\pi^2 \hbar c}{240 a^4} \quad (\text{Casimir, 1948})$$

For real metal plates the Casimir pressure is expressed by the Lifshitz formula via $\epsilon(\omega)$ (Lifshitz, 1955).

--- The predictions of the Lifshitz theory are excluded by the results of high-precision experiments if $\epsilon(\omega)$ is described by the well-established Drude model.

--- The same predictions come into conflict with thermodynamics.

These problems are known as the Casimir puzzle.



2D material

For graphene the electromagnetic response at low energies can be calculated on the basis of first principles of QED.

As a result:

- The predictions of the Lifshitz theory are in agreement with high-precision experiments.
- The same predictions satisfy the Nernst heat theorem.

In this talk, we consider:

- the role of s-polarized evanescent waves in the Casimir puzzle;
- possible solution of the Casimir puzzle using the lessons of graphene;
- new independent test of the Drude model in the range of low-frequency s-polarized evanescent waves.



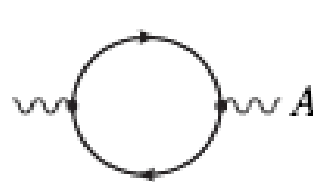
2. RESPONSE FUNCTIONS OF GRAPHENE AT LOW ENERGIES

At energies < 3 eV graphene is well-described by the Dirac model as a set of electronic quasiparticles interacting with electromagnetic field

$$\left[\tilde{\gamma}^0 \left(i\hbar \frac{\partial}{\partial t} - eA_0 - \mu \right) + \tilde{\gamma}^1 \left(i\hbar c \frac{\partial}{\partial x^1} - eA_1 \right) + \tilde{\gamma}^2 \left(i\hbar c \frac{\partial}{\partial x^2} - eA_2 \right) - \frac{\Delta}{2} \right] \psi(x) = 0,$$

where $\tilde{\gamma}^0 = \gamma^0$, $\tilde{\gamma}^{1,2} = \tilde{v}_F \gamma^{1,2}$, $\tilde{v}_F = \frac{v_F}{c}$, $\Delta = 2mv_F^2$, $x^\beta = (ct, x^1, x^2)$

An interaction of graphene with electromagnetic field is described by the diagram



with (q_0, \vec{q}_\perp) and (k_0, \vec{k}_\perp) -- the 3-component wave vectors of a loop electronic excitation and an external photon.



The respective polarization tensor at nonzero temperature is given by

$$\Pi^{\beta\delta}(k_{0l}, \vec{k}_{\perp}) = -8\pi\alpha k_B T \sum_{n=-\infty}^{\infty} \left(n + \frac{1}{2}\right) \int \frac{d^2\vec{q}_{\perp}}{(2\pi)^2} \\ \times \text{tr} \left[S(q_{0n}, \vec{q}_{\perp}) \tilde{\gamma}^{\beta} S(q_{0n} - k_{0l}, \vec{q}_{\perp} - \vec{k}_{\perp}) \tilde{\gamma}^{\delta} \right], \quad \text{where } \alpha = \frac{e^2}{\hbar c}.$$

In the Matsubara formalism

$$q_{0n} = 2\pi i \left(n + \frac{1}{2}\right) \frac{k_B T}{\hbar c}, \quad k_{0l} = \frac{i\xi_l}{c} = 2\pi i l \frac{k_B T}{\hbar c},$$

and the propagator of the quasiparticles takes the form

$$S(q_0, \vec{q}_{\perp}) = -\frac{\tilde{\gamma}^0 [q_0 + \mu/(\hbar c)] - \tilde{\gamma}^1 q_1 - \tilde{\gamma}^2 q_2 - \Delta/(2\hbar c)}{[q_0 + \mu/(\hbar c) + i\epsilon \text{sign} q_0]^2 - \tilde{v}_F^2 q_{\perp}^2 - \Delta^2/(4\hbar^2 c^2)}$$

[Fialkovsky, Marachevsky, Vassilevich, PRB 84, 035446 (2011);
Bordag, Fialkovsky, Vassilevich, PRB 93, 075414 (2017)]



The polarization tensor is defined by two independent quantities:

$$\Pi_{00}(i\xi_l, k_\perp) \equiv \Pi_{00,l},$$

$$\Pi(i\xi_l, k_\perp) \equiv k_\perp^2 \Pi_\beta^\beta(i\xi_l, k_\perp) - q_l^2 \Pi_{00}(i\xi_l, k_\perp) \equiv \Pi_l, \quad q_l^2 = k_\perp^2 + \frac{\xi_l^2}{c^2}.$$

It is convenient to present them as the sum of two contributions

$$\Pi_{00}(i\xi_l, k_\perp, T, \Delta, \mu) = \Pi_{00}^{(0)}(i\xi_l, k_\perp, \Delta) + \Pi_{00}^{(1)}(i\xi_l, k_\perp, T, \Delta, \mu),$$

$$\Pi(i\xi_l, k_\perp, T, \Delta, \mu) = \Pi^{(0)}(i\xi_l, k_\perp, \Delta) + \Pi^{(1)}(i\xi_l, k_\perp, T, \Delta, \mu).$$

Here,
$$\Pi_{00,l}^{(0)} = \frac{\alpha \hbar c k_\perp^2}{p_l} \Psi(D_l), \quad \Pi_l^{(0)} = \alpha \hbar k_\perp^2 \frac{p_l}{c} \Psi(D_l),$$

$$p_l^2 = v_F^2 k_\perp^2 + \xi_l^2, \quad D_l = \frac{\Delta}{\hbar p_l}, \quad \Psi(x) = 2 [x + (1 - x^2) \arctan(x^{-1})].$$

[Bordag, Fialkovsky, Gitman, Vassilevich, PRB 80, 245406 (2009)]



The contributions depending on chemical potential and temperature are more complicated:

$$\Pi_{00,l}^{(1)} = \frac{4\alpha\hbar c p_l}{v_F^2} \int_{D_l}^{\infty} du \left(\frac{1}{e^{B_l u + \frac{\mu}{k_B T}} + 1} + \frac{1}{e^{B_l u - \frac{\mu}{k_B T}} + 1} \right) \times \left[1 - \operatorname{Re} \frac{1 - u^2 + 2i \frac{\xi_l}{p_l} u}{\left(1 - u^2 + 2i \frac{\xi_l}{p_l} u + \frac{v_F^2 k_{\perp}^2}{p_l^2} D_l^2 \right)^{1/2}} \right],$$

$$\Pi_l^{(1)} = -\frac{4\alpha\hbar p_l \xi_l^2}{c v_F^2} \int_{D_l}^{\infty} du \left(\frac{1}{e^{B_l u + \frac{\mu}{k_B T}} + 1} + \frac{1}{e^{B_l u - \frac{\mu}{k_B T}} + 1} \right) \times \left[1 - \operatorname{Re} \frac{1 - \frac{p_l^2}{\xi_l^2} u^2 + 2i \frac{p_l}{\xi_l} u + \frac{v_F^2 k_{\perp}^2}{\xi_l^2} D_l^2}{\left(1 - u^2 + 2i \frac{\xi_l}{p_l} u + \frac{v_F^2 k_{\perp}^2}{p_l^2} D_l^2 \right)^{1/2}} \right],$$

$$\text{where } B_l = \frac{\hbar p_l}{2k_B T}.$$

[Bordag, Klimchitskaya, Mostepanenko, Petrov, PRD 91, 045037 (2015);
Bordag, Vialkovsky, Vassilevich, PRB 93, 075414 (2017);
Bimonte, Klimchitskaya, Mostepanenko, PRB 96, 115430 (2017)]



3. THE CASIMIR FORCE IN GRAPHENE SYSTEMS

The Casimir pressure between two graphene sheets is given by the Lifshitz formula:

$$P = -\frac{k_B T}{\pi} \sum_{l=0}^{\infty} ' \int_0^{\infty} q_l k_{\perp} dk_{\perp} \left\{ \left[r_p^{-2}(i\xi_l, k_{\perp}) e^{2aq_l} - 1 \right]^{-1} + \left[r_s^{-2}(i\xi_l, k_{\perp}) e^{2aq_l} - 1 \right]^{-1} \right\},$$

where the reflection coefficients are expressed via the polarization tensor of graphene

$$r_p(i\xi_l, k_{\perp}) = \frac{q_l \Pi_{00}(i\xi_l, k_{\perp})}{q_l \Pi_{00}(i\xi_l, k_{\perp}) + 2\hbar k_{\perp}^2},$$
$$r_s(i\xi_l, k_{\perp}) = -\frac{\Pi(i\xi_l, k_{\perp})}{\Pi(i\xi_l, k_{\perp}) + 2\hbar k_{\perp}^2 q_l}$$



The polarization tensor is equivalent to the spatially nonlocal dielectric permittivities

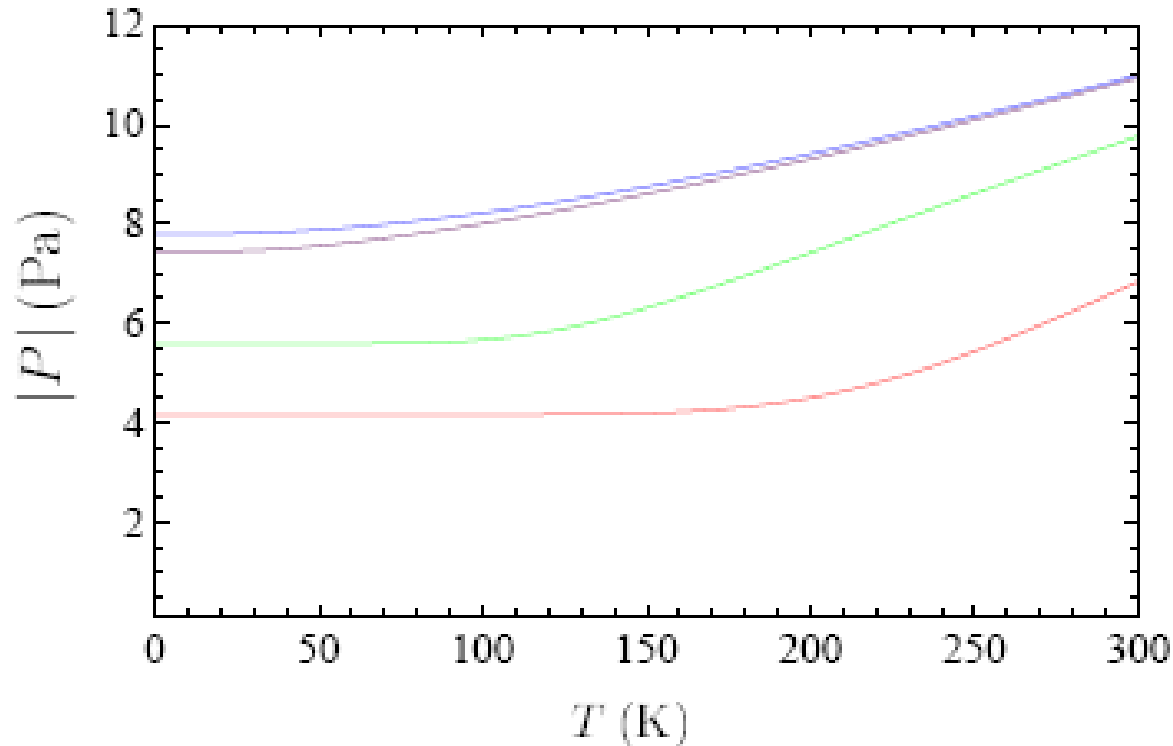
$$\varepsilon_{\text{long}}(i\xi_l, k_{\perp}) = 1 + \frac{1}{2\hbar k_{\perp}} \Pi_{00}(i\xi_l, k_{\perp}),$$

$$\varepsilon_{\text{tr}}(i\xi_l, k_{\perp}) = 1 + \frac{c^2}{2\hbar k_{\perp} \xi_l^2} \Pi(i\xi_l, k_{\perp}).$$

[Klimchitskaya, Mostepanenko, Sernelius, PRB 89, 125407 (2014)]

The Lifshitz theory predicts big thermal effect in the Casimir pressure between two graphene sheets already at separations of a few tens of nanometers

[Gomez-Santos, PRB 80, 245424 (2009)]



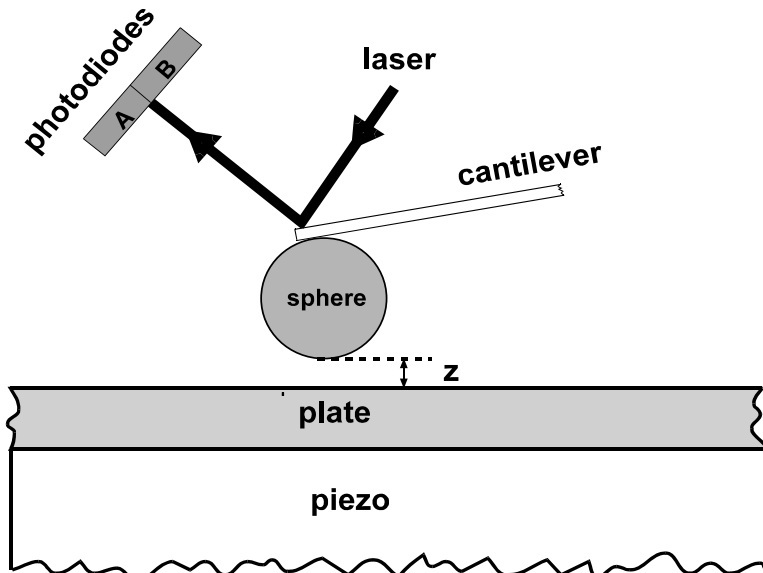
Temperature dependence at separation 30nm

Lines from bottom to top are for the mass gap parameters 0.1eV, 0.05eV, 0.01eV, and 0eV, respectively.



4. AGREEMENT BETWEEN EXPERIMENT AND THEORY IN GRAPHENE SYSTEMS

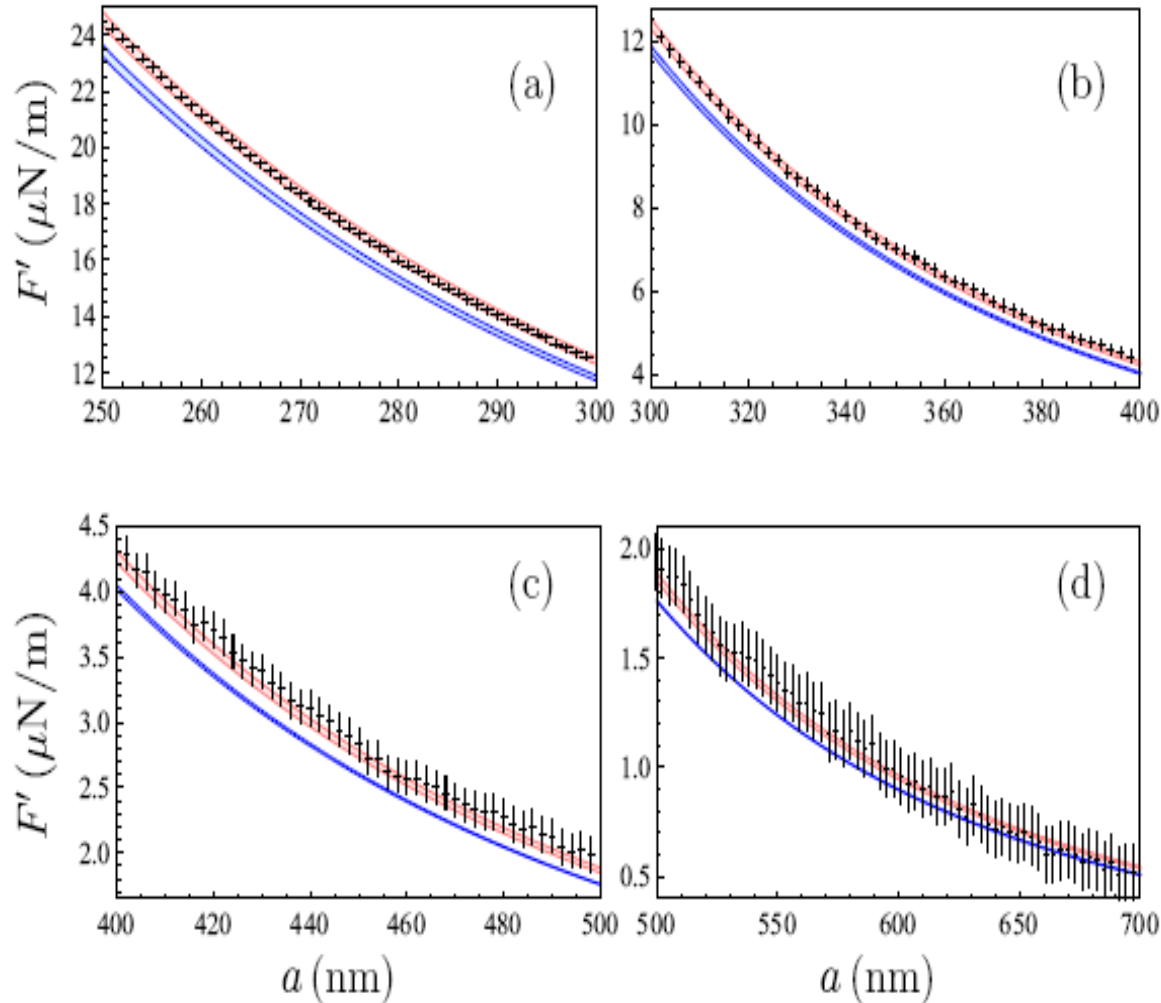
The gradient of the Casimir force was measured between an Au-coated glass microsphere and a graphene-coated fused silica plate by means of an atomic force microscope



Schematic diagram of the experimental setup using an atomic force microscope



Comparison between experiment and theory



The mean gradient of the Casimir force is shown by the crosses as a function of separation within four separation intervals. The red and blue bands are computed at the laboratory temperature 294K and at 0K, respectively

[Liu, Zhang, Klimchitskaya, Mostepanenko, Mohideen, PRL 126, 206802 (2021); PRB 104, 085436 (2021)]



5. AGREEMENT WITH THE REQUIREMENTS OF THERMODYNAMICS

The behavior of the Casimir entropy computed by the Lifshitz theory using the polarization tensor of graphene depends on the relationship between Δ and 2μ .

For $\Delta > 2\mu \geq 0$,
$$S(a, T) \sim \frac{k_B(k_B T)^4}{(\hbar c)^2 \Delta^2},$$

which is valid at $k_B T \ll \Delta - 2\mu$.

For $2\mu > \Delta \geq 0$,
$$S(a, T) \sim \frac{a(4\mu^2 - \Delta^2)k_B^2 T}{(\hbar c)^3},$$

which is valid at $k_B T \ll 2\mu - \Delta$.



For $\Delta = \mu = 0$, $S(a, T) \sim -k_B \left(\frac{k_B T}{\hbar c} \right)^2 \ln \frac{a k_B T}{\hbar c}$,

which is valid at $k_B T \ll \frac{\hbar v_F}{2a}$.

[Bezerra, Klimchitskaya, Mostepanenko, Romero, PRA 94, 042501 (2016)]

For $\Delta = 2\mu \neq 0$, $S(a, T) \sim \frac{k_B}{a^2}$.

The Nernst heat theorem is followed in all cases with exception of only the exact equality $\Delta = 2\mu \neq 0$, which cannot be realized for real graphene sheet.

[Klimchitskaya, Mostepanenko, PRD 102, 016006 (2020)]

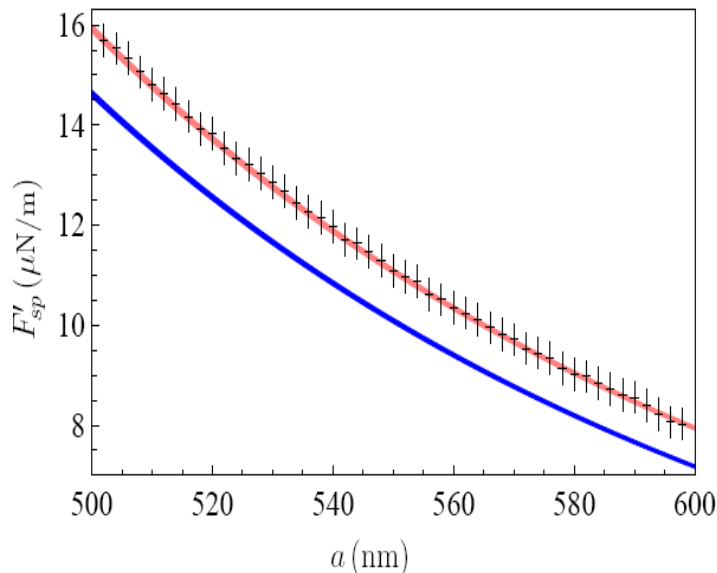


6. WHAT IS THE CASIMIR PUZZLE FOR METALLIC PLATES?

Predictions of the Lifshitz theory **agree** with the measurement data if the low-frequency response of metals is described by the dissipationless **plasma model** but are **excluded** if the dissipative **Drude model** is used

$$\epsilon_{pl}(\omega) = 1 - \frac{\omega_p^2}{\omega^2}$$

$$\epsilon_D(\omega) = 1 - \frac{\omega_p^2}{\omega(\omega + i\gamma)}$$

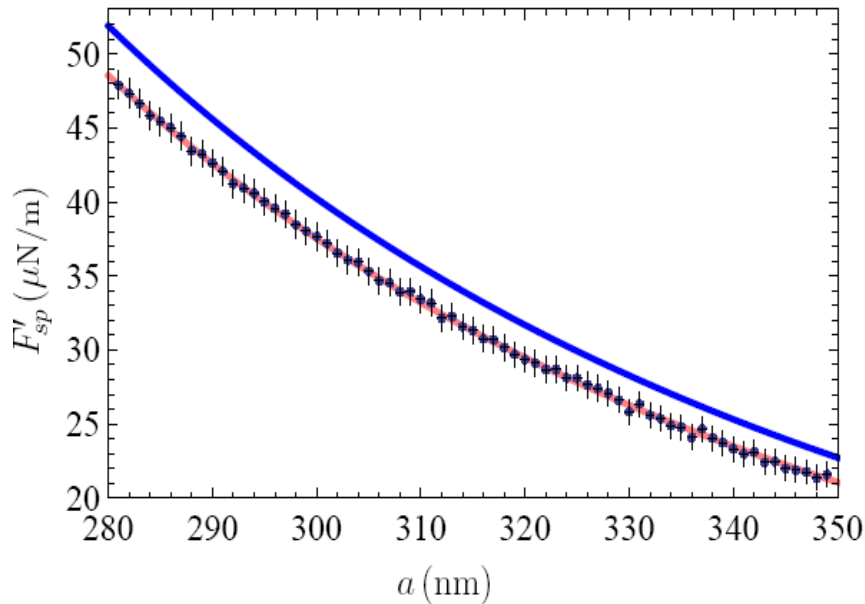


The gradients of the Casimir force between an Au-coated sphere and an Au-coated plate measured by means of micromechanical torsional oscillator (crosses) are compared with predictions of the Lifshitz theory using the Drude and plasma extrapolations of the optical data of Au (blue and red bands, respectively).

[Decca, Lopez, Fischbach, Klimchitskaya, Krause, Mostepanenko, PRD 75, 077101 (2007)]



For the magnetic test bodies the theoretical predictions of the Drude and plasma models exchange places



The gradients of the Casimir force between a Ni-coated sphere and a Ni-coated plate measured by means of dynamic atomic force microscope (crosses) are compared with predictions of the Lifshitz theory using the Drude and plasma extrapolations of the optical data of Ni (blue and red bands)

[Banishev, Klimchitskaya, Mostepanenko, Mohideen, PRL 110, 137401 (2013)]

In the differential measurement, the experimentally confirmed force-signal calculated using the plasma model differs by up to a factor of 1000 from the excluded signal calculated using the Drude model.

[Bimonte, Lopez, Decca, PRB 93, 184434 (2016)]



Theoretically, for metallic plates with perfect crystal lattices, which is an equilibrium system, the Casimir entropy calculated using the Drude model violates the Nernst heat theorem:

$$S_D(a, 0) = -\frac{k_B \zeta(3)}{16\pi a^2} \left[1 - 4\frac{\delta_0}{a} + 12\left(\frac{\delta_0}{a}\right)^2 - \dots \right] < 0, \quad \delta_0 = \frac{c}{\omega_p}.$$

If the plasma model is used,

$$\lim_{T \rightarrow 0} S_{pl}(a, T) = S_{pl}(a, 0) = 0,$$

i.e., the Nernst heat theorem is satisfied.

[Bezerra, Klimchitskaya, Mostepanenko, Romero, PRA 69, 022119 (2004)]



7. THE ROLE OF s-POLARIZED EVANESCENT WAVES IN THE CASIMIR PUZZLE

At $a \geq 6 \mu\text{m}$ the Casimir pressure predicted by the Drude and plasma models differs by a factor of 2:

$$P_D(a, T) = -\frac{k_B T}{8\pi a^3} \zeta(3), \quad P_{pl}(a, T) = -\frac{k_B T}{4\pi a^3} \zeta(3).$$

The total pressure can be presented as a sum of contributions

from the propagating waves for which $k_{\perp} < k_0 = \frac{\omega}{c}$
and evanescent waves ($k_{\perp} > k_0$)

$$P(a, T) = P^{\text{prop}}(a, T) + P^{\text{evan}}(a, T).$$



At separations $a \gg \frac{\hbar c}{2k_B T}$ (i.e., at $a > 6 \mu\text{m}$, $T = 300 \text{ K}$)
one has:

$$P^{\text{prop}}(a, T) = \frac{k_B T}{\pi^2} \int_0^\infty \frac{d\omega}{\omega} \\ \times \int_0^{k_0} dk_\perp k_\perp \tilde{q} \sum_\sigma \text{Re} \frac{r_\sigma^2(\omega, k_\perp) e^{2ia\tilde{q}}}{1 - r_\sigma^2(\omega, k_\perp) e^{2ia\tilde{q}}},$$
$$P^{\text{evan}}(a, T) = -\frac{k_B T}{\pi^2} \int_0^\infty \frac{d\omega}{\omega} \\ \times \int_{k_0}^\infty dk_\perp k_\perp q \sum_\sigma \text{Im} \frac{r_\sigma^2(\omega, k_\perp) e^{-2aq}}{1 - r_\sigma^2(\omega, k_\perp) e^{-2aq}}.$$

Here, $\sigma = (p, s)$, $q = \sqrt{k_\perp^2 - k_0^2}$, $\tilde{q} = \sqrt{k_0^2 - k_\perp^2}$.



If the Drude model is used:

$$P_{D,s}^{\text{prop}}(a, T) = -\frac{k_B T}{8\pi a^3} \zeta(3), \quad P_{D,s}^{\text{evan}}(a, T) = \frac{k_B T}{8\pi a^3} \zeta(3),$$

$$P_{D,p}^{\text{prop}}(a, T) = -\frac{k_B T}{8\pi a^3} \zeta(3), \quad P_{D,p}^{\text{evan}}(a, T) = 0.$$

[Svetovoy, Esquivel,
J. Phys. A 39, 6777 (2006)]

For the plasma model it holds:

$$P_{pl,s}^{\text{prop}}(a, T) = -\frac{k_B T}{8\pi a^3} \zeta(3), \quad P_{pl,s}^{\text{evan}}(a, T) = 0,$$

$$P_{pl,p}^{\text{prop}}(a, T) = -\frac{k_B T}{8\pi a^3} \zeta(3), \quad P_{pl,p}^{\text{evan}}(a, T) = 0.$$

Thus, the total difference between the theoretical predictions obtained using the Drude and plasma models is fully determined by the contribution of s-polarized evanescent waves.



8. THE LESSONS OF GRAPHENE FOR THE CASIMIR PUZZLE

Why the Lifshitz theory is in agreement with the measurement data for graphene and is in disagreement with the data for metals described by the well-established Drude model?

The response functions of graphene at low energies, contributing to the Casimir force at the experimental separations, were derived **on the basis of first principles of QED.**

They are spatially nonlocal and applicable to both the propagating and evanescent waves

$$\left(\text{i.e., for } \frac{\omega}{c} > k_{\perp} \text{ and } \frac{\omega}{c} < k_{\perp} \right)$$



By contrast, the Drude model is of phenomenological character.
The most of its confirmations belong to the area of propagating waves.

--- Physics of surface plasmon polaritons provides confirmation of the Drude model in the area of evanescent waves with large k_{\perp} but only for the p-polarization

[Torma, Barnes, Rep. Progr. Phys. 78, 013901 (2015)].

--- Total internal reflection and frustrated total internal reflection allow to probe the region of k_{\perp} only slightly exceeding ω/c

[Zhu, Hawley, Roy, Am. J. Phys. 54, 601 (1986)].

--- The near field optical microscopy is more sensitive to the p-polarized evanescent waves

[Aigouy et al., Opt. Lett. 24, 187 (1999)].



This means that the Drude model is lacking of confirmation in the region of extremely evanescent s-polarized fields $\left(k_{\perp} \gg \frac{\omega}{c}\right)$ which are responsible for the Casimir puzzle for metallic test bodies.

Based on this, the phenomenological spatially nonlocal permittivity was proposed

$$\varepsilon^{\text{Tr}}(\omega, \vec{k}) = 1 - \frac{\omega_p^2}{\omega(\omega + i\gamma)} \left(1 + i \frac{v^{\text{Tr}} k}{\omega}\right), \text{ where } k = |\vec{k}|, \quad v^{\text{Tr}} = 1.5v_F$$

This permittivity nearly coincides with the Drude model for the propagating waves but deviates from it for the evanescent waves.

[Klimchitskaya, Mostepanenko, Eur. Phys. J. C 80, 900 (2020);
PRD 104, 085001 (2021)]



The phenomenological permittivity takes into account the dissipation of conduction electrons and simultaneously brings theoretical predictions of the Lifshitz theory in agreement with all precise experiments on measuring the Casimir force.

[Klimchitskaya, Mostepanenko, PRA 105, 012805 (2022)]

The Casimir entropy calculated using this permittivity satisfies the Nernst heat theorem.

[Klimchitskaya, Mostepanenko, PRD 104, 085001 (2021)]

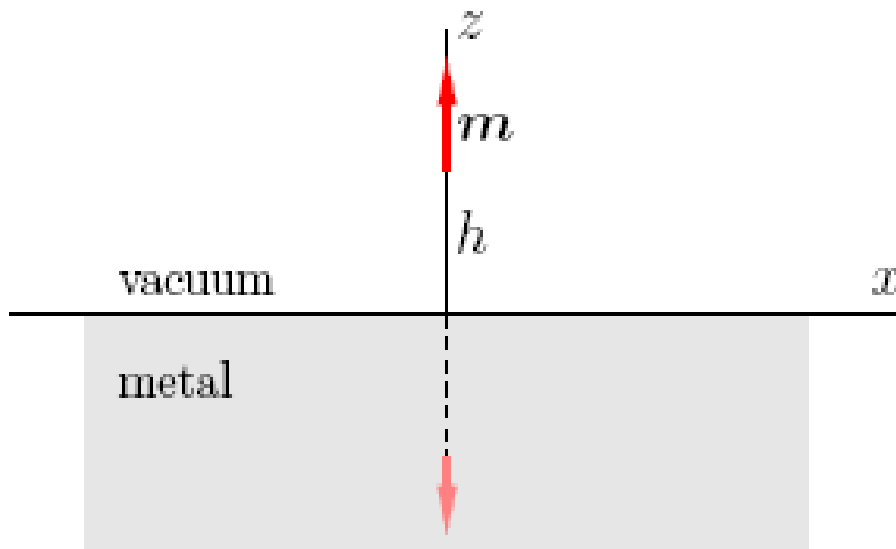
The question arises:

Is it possible to independently check the validity of the Drude model in the range of low-frequency s-polarized evanescent waves?

9. TESTING THE DRUDE MODEL IN THE RANGE OF s-POLARIZED EVANESCENT WAVES



Recently it was found that the magnetic field of an oscillating magnetic dipole spaced above a thick metallic plate is in many ways similar to the Casimir force at large separations considered in Sec. 6.



Magnetic dipole above thick metallic plate and image dipole.

$$\vec{m} = (0, 0, m_0 e^{-i\omega t})$$



Under a condition, that the dipole size is much smaller than the wavelength of oscillations, the components of the magnetic field were derived by the method of images and by the Green function method with the coinciding results

$$H_x^{(p)}(\omega, \vec{r}) = \frac{m_0 x}{\rho} \int_{k_0}^{\infty} dk_{\perp} k_{\perp}^2 J_1(k_{\perp} \rho) r_s(\omega, k_{\perp}) e^{-\sqrt{k_{\perp}^2 - k_0^2}(z+h)} - m_0 \frac{x(z-h)}{r^2} \left(\frac{k_0^2}{r} + 3i \frac{k_0}{r^2} - \frac{3}{r^3} \right) e^{ik_0 r},$$

similar expression for $H_y^{(p)}(\omega, \vec{r})$ with $x \rightarrow y$,

$$H_z^{(p)}(\omega, \vec{r}) = m_0 \int_{k_0}^{\infty} dk_{\perp} \frac{k_{\perp}^3}{\sqrt{k_{\perp}^2 - k_0^2}} J_0(k_{\perp} \rho) r_s(\omega, k_{\perp}) e^{-\sqrt{k_{\perp}^2 - k_0^2}(z+h)} + m_0 \left[\frac{k_0^2}{r} + i \frac{k_0}{r^2} - \frac{1}{r^3} - \frac{(z-h)^2}{r^2} \left(\frac{k_0^2}{r} + 3i \frac{k_0}{r^2} - \frac{3}{r^3} \right) \right] e^{ik_0 r},$$

where $r = \sqrt{\rho^2 + z^2}$, $\rho^2 = x^2 + y^2$.



Let us consider the lateral field component along the x-axis at $z=h$

$$H_x^{(p)}(\omega, \vec{r}) = \frac{m_0 x}{\rho} \int_{k_0}^{\infty} dk_{\perp} k_{\perp}^2 J_1(k_{\perp} \rho) r_x(\omega, k_{\perp}) e^{-\sqrt{k_{\perp}^2 - k_0^2}(z+h)}$$

For typical experimental parameters $h \sim 1$ cm, $\omega \sim 100$ rad/s
the contribution of propagating waves

is suppressed by the factor $(k_0 h)^3 \sim 10^{-27}$.

The electric field of the dipole

is suppressed by the factor $k_0 h \sim 10^{-9}$.

The oscillating magnetic dipole can be realized as a 1-mm coil

$$m_0 = \frac{1}{c} \pi N I_0 R^2 \quad \text{with } N = 10, \quad I_0 = 1 \text{ A}, \quad R = 1 \text{ mm}$$

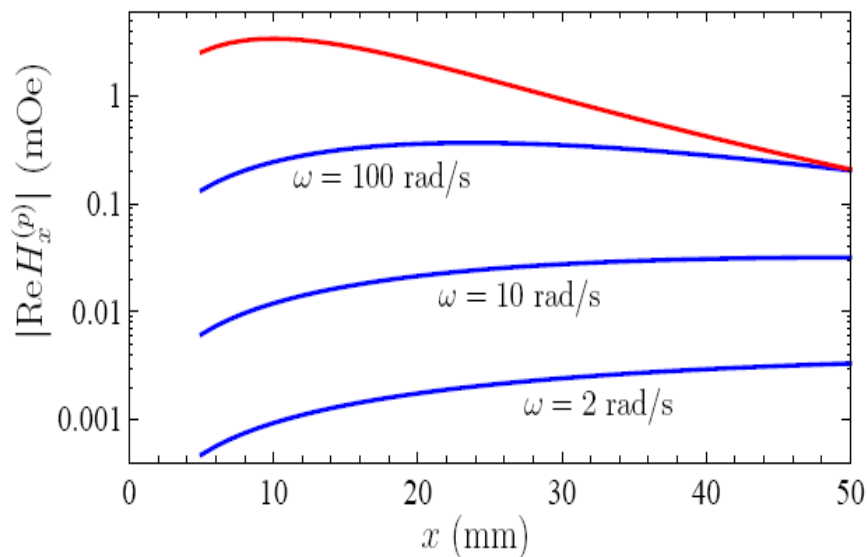
leading to

$$m_0 = 3.14 \times 10^{-2} \text{ erg/Oe} = 3.14 \times 10^{-5} \text{ A m}^2$$

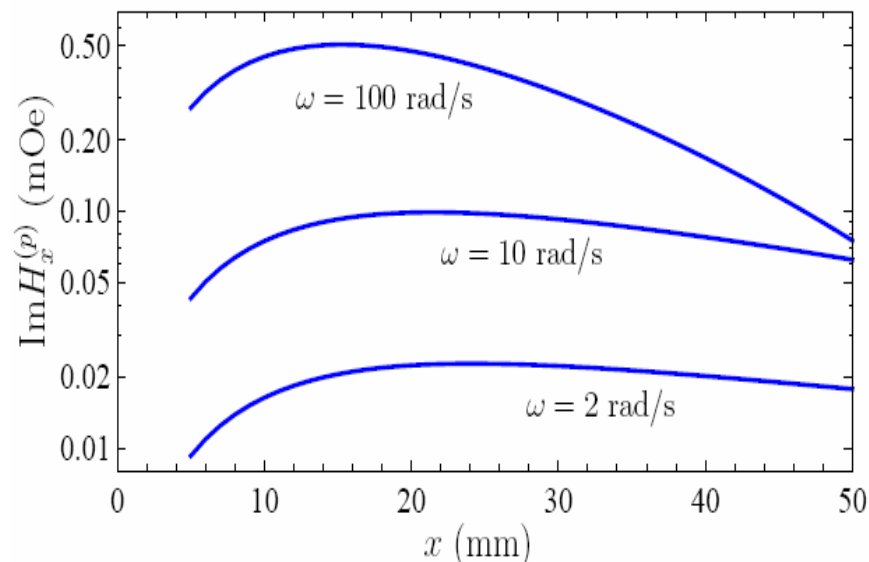


The computational results are:

(a)



(b)



The three lines counted from bottom are computed using the Drude model and the top line (a) using the plasma model or the spatially nonlocal model. For the plasma model $\text{Im}H_x^{(p)} = 0$.

These figures clearly demonstrate that by measuring the lateral component of the magnetic field one can either confirm or exclude the validity of the Drude model as a response function to the low-frequency s-polarized evanescent waves.



10. CONCLUSIONS

I. The response function of a material is the central concept of fluctuational electrodynamics and it is desirable to have reliable information about it.



II. High-precision measurements of the Casimir force cast serious doubts upon the validity of the Drude model in the range of low-frequency s-polarized evanescent fields.



III. Similar measurements with graphene systems are in a very good agreement with theoretical predictions of the Lifshitz theory using the spatially nonlocal response functions found on the basis of first principles of QED.



IV. We propose the decisive independent experimental test which will show whether or not the Drude model is applicable in the range of low-frequency s-polarized evanescent fields.